Weighted Recursive Graph Color Coding for Enhanced Load Identification

Li Zhang, Hengtao Ai, Yuhang Liu, Shiqing Li, Tao Zhang*
School of Electrical Engineering and Automation, Henan Polytechnic University, Jiaozuo, China[1, 2, 3, 4, 5]
Henan Key Laboratory of Intelligent Detection and Control of Coal Mine Equipment, Jiaozuo, China[1]
Henan International Joint Laboratory of Direct Drive and Control of Intelligent Equipment, Jiaozuo, China[5]

***Abstract*—In the pursuit of high-precision load identification, traditional methodologies grapple with significant drawbacks, including low recognition rates, intricate signature construction, and narrow applicability. This study introduces a novel approach employing weighted recursive graph (WRG) color coding to surmount these challenges. Power consumption data, procured from advanced load monitoring devices, undergo extraction of single-cycle currents, which are then subjected to dimensional reduction via Piece-wise Aggregate Approximation (PAA). In a transformative step, these currents are encoded into load signatures through the recursive graph time series methodology, culminating in the generation of WRG images. An AlexNet neural network model is engaged to distil and assimilate the distinctive features of the WRG images. The simulation results indicate that the identification rate can exceed 97%. Additionally, an experimental platform was set up to verify the method proposed in this paper, and the results show that the actual identification rate can reach over 96%. Both the simulation results and experiments fully demonstrate that the proposed identification method has a high accuracy. This method not only sets a new standard in non-intrusive load identification but also enhances the generalization of load signature applicability across diverse scenarios.**

***Keywords*—Non-Intrusive Load Monitoring (NILM); Weighted Recurrence Graph (WRG); color coding; AlexNet neural network; load signature**

I. Introduction

In pursuit of the ambitious "dual carbon" objectives and the establishment of innovative electric power systems, the crafting of an energy infrastructure that is clean, carbon-efficient, secure, and effective has been deemed essential to the evolution of power grids [1]. The technology for load identification has been recognized as a crucial facilitator for these emergent power systems, holding a key position in the attainment of automated demand response mechanisms. The precision in identifying electrical loads at the point of consumption is imperative for the enhancement of energy consumption management. The methodology for load identification bifurcates into two distinct approaches contingent upon the mode of power data procurement: Intrusive Load Monitoring (ILM) and Non-Intrusive Load Monitoring (NILM) [2]. Owing to its cost-effective nature, streamlined communication, and ease of maintenance and scalability, NILM has gained prominence as the preferred method for load identification [3].

A plethora of studies have delved into load identification methods based on NILM in recent years. Traditional identification techniques, such as the K-Nearest Neighbor algorithm [4], Support Vector Machine [5], Decision Trees, and Random Forests [6], were widely adopted in earlier research. These initial methods, while computationally less demanding, focused primarily on frequency and phase of electrical data and other load characteristics, resulting in lower accuracy rates. With the advent of deep learning, which has demonstrated remarkable success in image classification and object detection, researchers have turned to two-dimensional visualization of time series data [7]. By transforming time-series problems into image classification tasks within the realm of image recognition, these methods have seen a substantial improvement in identification rates compared to their predecessors [8]. However, when the load types and characteristics are similar, there is an issue of identification confusion. One of the earliest methods to visualize electrical signals as images in the NILM field was through V-I trajectories [9]. Building on this, Taha Hassan et al. proposed using instantaneous voltage and current to construct V-I trajectories, replacing traditional load characteristics and significantly improving the accuracy and reliability of load identification [10]. Methods such as those in Literature [11], which employ grayscale voltage-current (V-I) trajectory construction, are pioneering yet suffer from low identification rates due to poor image resolution and the absence of color information. Subsequently, Literature [12] introduced color-coded V-I trajectories as load signatures, enhancing identification accuracy; however, the complexity of constructing these signatures limited their widespread applicability. To address the shortcoming of V-I trajectories that do not reflect the power magnitude of electrical devices, study in [13] proposed a method that integrates V-I trajectories with power features, improving the precision of load identification. Nevertheless, this method still faces challenges in identifying complex loads, resulting in lower success rates.

In summary, current load identification methods face the issue of low identification rates when handling large amounts of load data. Therefore, based on previous research [3], this paper adopts image recognition methods to process large-scale loads. In consideration of the dependency on complex load signatures for achieving high-precision load identification, this study introduces a load identification method employing WRG color coding. To simplify the acquisition of load signatures, the processed electrical currents from power devices are transformed into WRG images through an improved recursive graph color coding technique. The superiority and effectiveness of the method proposed herein are comprehensively validated using an enhanced AlexNet neural network on the PLAID and WHITED datasets, as well as empirical data gathered in a laboratory environment. This demonstrates that the proposed method not only reduces the difficulty of acquiring load data but also improves the accuracy of load identification. It provides technical support for achieving high-precision load identification for residential users and offers a means for their participation in demand response.

II. Principles of Load Identification

NILM technique facilitates the real-time monitoring of the type, operational status, and energy consumption of user-side electrical devices through the deployment of intelligent load collection devices at the entrance of the electrical system. These devices process and analyze the collected electrical data. This technology is comprised of three principal modules: data acquisition, feature extraction, and load identification (see Fig. 1) [14]. The specific process of the method proposed in the study is outlined as follows:

1) Acquisition phase: Intelligent sensing devices are deployed to capture high-frequency voltage and current data from electrical apparatuses. Subsequently, these data are subjected to a preprocessing protocol, the objective of which is to distill the information into single-cycle waveform representations of voltage and current.

2) Feature reduction and extraction phase: Employing PAA [15], the single-cycle current waveform undergoes a dimensionality reduction process. This is succeeded by the application of a weighted recurrence graph encoding methodology, culminating in the generation of WRG, earmarked as the discriminative features for subsequent load identification.

3) Identification phase: The feature set, embodied by the WRG images, is then introduced into an AlexNet neural network model. This model undertakes the dual role of feature extraction and pattern learning, thereby fulfilling the process of load identification.

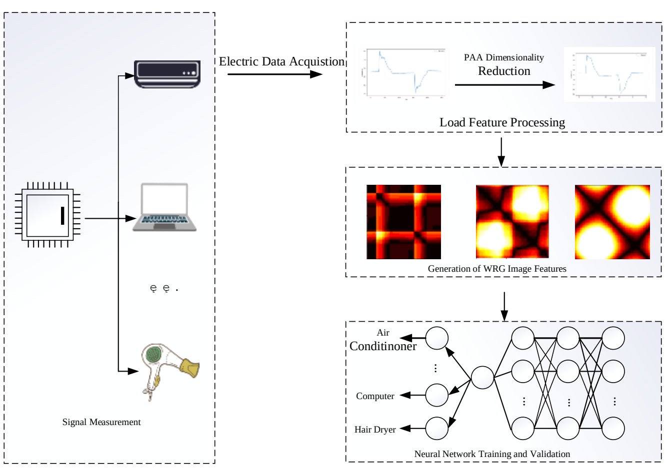

Fig. 1. Flow of load identification.

III. Load Data Processing and Modelling

A. Load Data Processing

For experimental validation, datasets from PLAID [16] and WHITED [17], both publicly available, were utilized, with data collected by high-frequency meters. The PLAID dataset comprises 1,074 records of current and voltage from 11 types of electrical appliances across 55 US households, with a sampling rate of 30kHz. The WHITED dataset encompasses 1,259 records from 54 types of electrical appliances from various regions worldwide, at a sampling rate of 44kHz. Each dataset exhibits distinctive characteristics: the PLAID data possesses high intra-class variation, while the WHITED dataset displays significant inter-class variation [18]. Thus, the data from these public datasets sufficiently meet the validation requirements of this study. However, considering the effectiveness in actual application scenarios, data measured in a laboratory environment are also introduced in subsequent sections to verify the practical applicability of the methods proposed herein.

According to study [19], the voltage and current waveforms of electrical appliances were extracted for several steady-state operating cycles before and after switching events. By referencing the fundamental voltage phase, a full-cycle average of the interpolated data was performed to obtain several cycles of steady-state voltage and current data preceding and following switching events, denoted as v_{off}, v_{on}, and i_{off}, i_{on} respectively. Given the consistent phase of voltage v_{off}, v_{on} and current i_{off}, i_{on} the voltage and current for an individual electrical load can be defined as $v(t) = (v_{off} + v_{on})/2$ and $i(t) = i_{off} - i_{on}$ respectively.

To simplify the load feature model and enhance the efficiency of algorithm execution, it is necessary to reduce the dimensionality of the current data. The PAA method was employed to diminish the dimensionality of the current to a pre-specified level. Furthermore, an analysis was conducted on the impact of different dimensionality reduction levels on the performance and learning speed of the AlexNet model in load identification tasks, with various parameters being adjusted for experimental analysis. Conclusions drawn from the results depicted in Fig. 2 indicate that the selection of parameters does not significantly affect the identification performance of the AlexNet model; however, it does have a notable impact on learning speed. Experimental validation confirmed that at a selected dimensionality $w = 50$, both identification accuracy and learning speed can be optimally balanced. Therefore, this dimensionality $w = 50$ was chosen for the reduction of load current dimensions.

B. Construction of Load Signatures

To further enhance the uniqueness of the current features of different types of loads, the method of WRG has been employed in this study for the color-coding of current data. Recurrence graphs are an effective method for analyzing the nonlinear dynamic characteristics of systems, capable of encoding one-dimensional time series into two-dimensional images, thereby revealing the chaos, stationarity, and inherent similarity of the time series, and enhancing feature extraction. Assuming that the electrical data constitutes a time series $x = \{x_1, x_2, \cdots, x_{Ts}\}$

containing T_s values, the specific steps for color-coding of the recurrence graph are as follows:

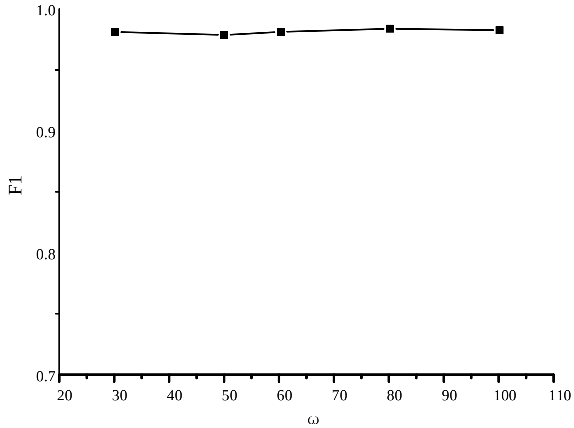

(a) Identification performance in case of different values of w

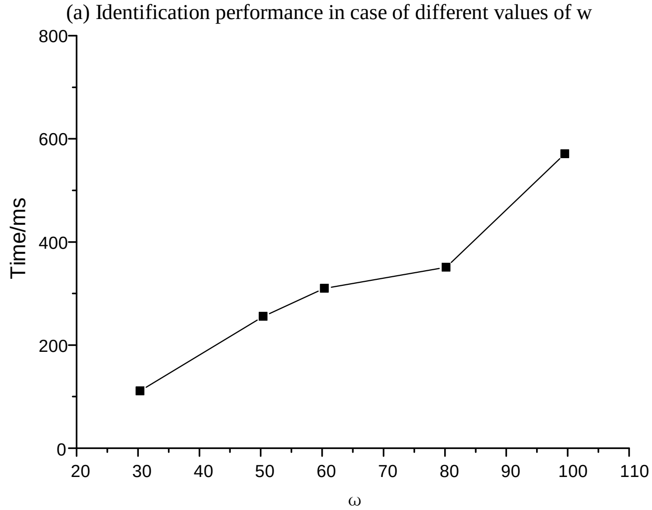

(b) Training time in case of different values of w

Fig. 2. Identification performance and training time in case of different values of w.

1) The similarity of distance $d_{k,j} = \|x_k - x_j\|^2$ between any two points x_k and x_j in $x = \{x_1, x_2, \cdots, x_{Ts}\}$ is calculated, where $d_{k,j}$ represents the Euclidean norm, then the distance similarity matrix $D_{w\times w}$ can be written as:

$$D_{w\times w} = \begin{bmatrix} d_{1,1} & \cdots & \cdots & \cdots & d_{1,j} \\ \vdots & \ddots & \cdots & \cdots & \vdots \\ \vdots & \cdots & \ddots & \cdots & \vdots \\ d_{k,1} & \cdots & \cdots & \ddots & d_{k,j} \end{bmatrix} \tag{1}$$

In classification tasks, distance threshold matrices are frequently employed. These matrices encapsulate all recursive relationships, articulating them as binary matrix $RG_{w\times w} = [r_{k,j}]$, where each element $r_{k,j}$ is defined as:

$$r_{k,j} = \begin{cases} 1 & d_{k,j} \geq \varepsilon \\ 0 & \text{otherwise} \end{cases} \tag{2}$$

where, $\varepsilon \in (0,1)$, representing the recurrence threshold. In the formula above, if the distance between two values in signal $x = \{x_1, x_{2,} \cdots, x_w\}$ is less than ε, then a point is plotted within the $w \times w$ grid.

2) Since the binarization of the distance matrix $D_{w\times w}$ through thresholding may lead to information loss and consequently decrease classification performance, the generation of $WRG_{w\times w}$ which surpasses the traditional binary output is introduced. This is achieved by incorporating parameter $\delta \geq 1$, allowing the values of $r_{k,j}$ to fall between 0 and δ, satisfying the following condition:

$$r_{k,j} = \begin{cases} \delta & \tau > \delta \\ \tau & \text{otherwise} \end{cases} \tag{3}$$

where, $\tau = \left\lfloor \frac{d_{k,j}}{\varepsilon} \right\rfloor$, $\lfloor \bullet \rfloor$ denotes the floor function. To ensure computational stability, the value of ε is parameterized with respect to 0 to ensure that $\lambda = 1/\varepsilon$. The matrix $D_{w\times w}$ can be interpreted as a weighted graph $G = (V, E)$, where each value represents the weight of an edge. Since $d_{k,j} > 0$, when $\delta \leq 1$, the equation can be simplified to RG. The recursive threshold ε and δ are hyperparameters that need to be optimized. Following the optimization of the recursive threshold, Fig. 3 illustrates the WRG images generated from residential load data collected in a laboratory setting.

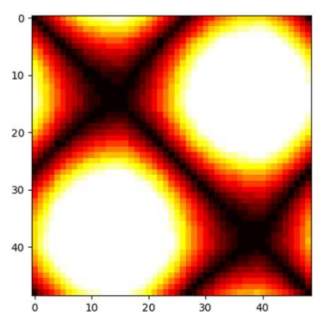

(a) Air conditioner

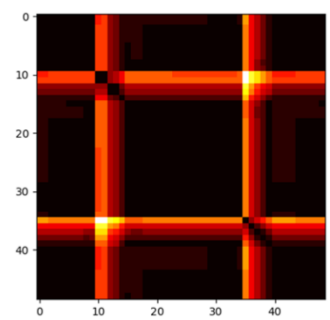

(b) Laptop

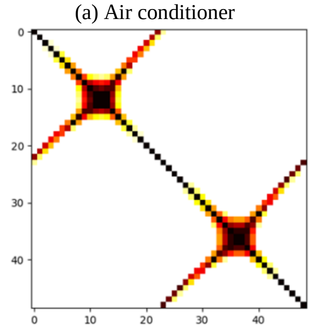

(c) Hair dryer

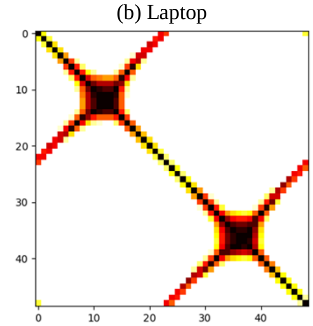

(d) Electric kettle

Fig. 3. WRG images of electrical apparatus measured in laboratory environment.

C. *Identification Algorithm*

In this study, the AlexNet neural network model is employed for the extraction and learning of features from WRG images to accomplish the task of load identification. The AlexNet neural network model comprises eight weighted layers, including five convolutional layers, three fully connected layers, and one softmax layer. The architecture of the network is delineated in Table I. Owing to the fact that the original AlexNet network model does not satisfy the classification requirements for experimental validation, adjusting the size of kernels and step size in the convolutional layers to accommodate the dimensions of the images to be classified.

Optimizations were implemented in the AlexNet neural network model to enhance its performance in load identification tasks from two aspects. Firstly, the Dropout layers within the AlexNet model were omitted to forestall the issue of overfitting. Secondly, adjustments were made to the number of neurons in the output layer to align with the specific demands of load identification tasks. Compared to the original model, the optimized AlexNet network model not only reduced the computational resource requirements for load identification tasks but also increased the accuracy of identification results.

TABLE I. STRUCTURE OF NEURAL NETWORK

Type	***Kernel Size***	***Step size***	***Output Dimension***
Convolutional Layer 1	11×11	4	96
Pooling Layer 1	3×3	2	-
Convolutional Layer 2	5×5	1	256
Pooling Layer 2	3×3	2	-
Convolutional Layer 3	3×3	1	384
Convolutional Layer 4	3×3	1	384
Convolutional Layer 5	3×3	1	256
Pooling Layer 3	3×3	2	256

D. *Evaluation Metrics*

In this study, a multi-dimensional analysis of the load identification results is conducted using confusion matrix [11], precision, recall, and F1-score.

The confusion matrix, also known as an error matrix, is a standard format representing accuracy assessment, presented in an n×n matrix form. Evaluation metrics such as overall precision, producer's precision, and user's precision are employed, reflecting different aspects of the accuracy of image classification.

Precision is defined as the ratio of correctly identified samples to the total number of samples in the test set, serving as an indicator of the overall identification performance of the test samples; recall is the proportion of samples accurately identified by the classification model out of all actual correct samples; the F1-score is utilized to assess the quality of identification for each class of electrical devices. The computational methods are as shown in Eq. (4) to (6).

$$P = \frac{T_P}{T_P + F_P} \tag{4}$$

$$R = \frac{T_P}{T_P + F_n} \tag{5}$$

$$F_1 = \frac{2 \times P \times R}{P + R} \tag{6}$$

where, P represents precision, R denotes recall, and F is the harmonic mean of precision and recall, serving as a comprehensive evaluation metric. $\boldsymbol{T_P}$ indicates the count of true positives, which are instances correctly predicted as positive; F_P stands for false positives, which are instances incorrectly predicted as positive despite being negative; F_n refers to false negatives, which are instances that are actually positive but have been incorrectly predicted as negative.

IV. CASE STUDY

A. *Experimental Setup*

As outlined in the preceding sections, the load identification process introduced in this study was validated using a combination of public datasets and actual measurement data. In the practical case study, a deep learning framework based on Python 3.9 and PyTorch, with hardware consisting of an NVIDIA RTX3060 and 16GB RAM, was employed.

The AlexNet neural network model was trained using Stochastic Gradient Descent (SGD), starting with a learning rate of 0.01, which was then reduced by a factor of 0.1 every 10 epochs; the batch size for training was set at 64, with the number of iterations fixed at 100.

The experimental part employed 10-fold cross-validation, a method used to assess the applicability of statistical analysis results to independent datasets. The original data were randomly divided into 10 subsets of equal size. Subsequently, 9 of these subsets were used as training data to train the model, with the remaining subset serving as the validation set for assessing the model's performance. This process was iterated 10 times to ensure a comprehensive evaluation of the model's performance. This method is beneficial for reducing uncertainties due to variations in dataset partitioning and for assessing the model's generalization ability.

B. *Dataset Experiments and Result Analysis*

Following the methodology for constructing load signatures introduced in Section III, the high-frequency current data from the PLAID and WHITED datasets were processed and transformed into WRG images using a weighted recursive method. These images were then input into the AlexNet neural network model for training and validation. Fig. 4 shows the training and verification results of AlexNet neural network model on PLAID and WHITED datasets.

The results of Fig. 4 show that the proposed method has good identification results in the two datasets, and the load identification rate in the PLAID dataset can reach 97%, and the load identification rate in the WHITED dataset can reach 98%. The results of the two datasets effectively prove the universality of the proposed method. The results indicate that for the WHITED dataset, which has a greater variety of load types, the identification rate is higher. This demonstrates the superiority of the proposed method when handling large-scale loads. However, it also shows that in scenarios with fewer load types, the advantage of the proposed method is not as significant.

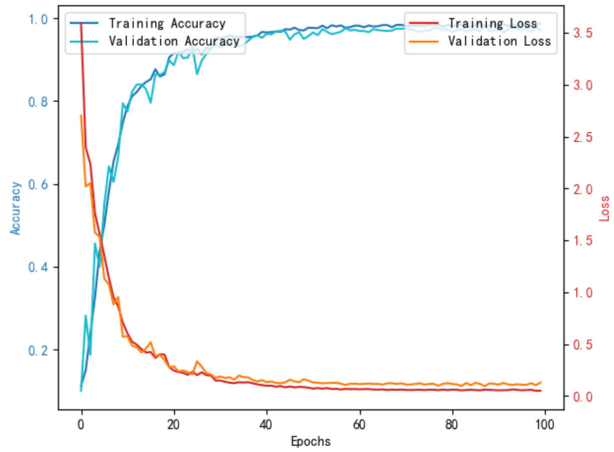

(a) PLAID dataset experimental results.

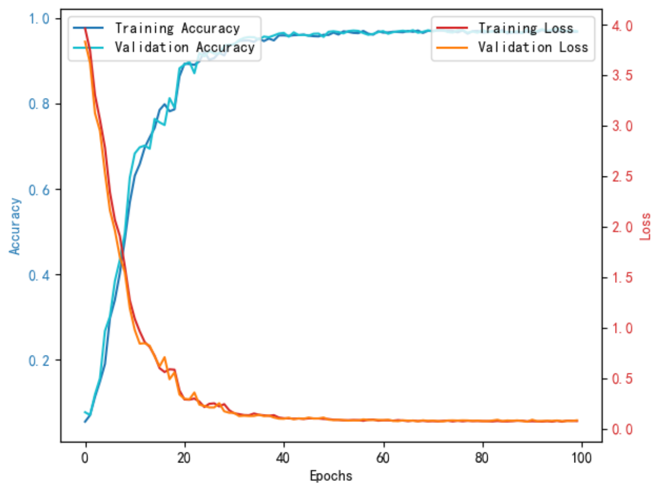

(b)WHITED dataset experimental results.

Fig. 4. WRG image example results.

The precision, recall, and F1-scores for each class within the PLAID dataset are presented in Table II. It can be observed that the precision, recall, and F1-scores for all 11 classes exceed 97%, with appliances such as fluorescent lamps, hairdryers, heaters, and vacuum cleaners achieving a 100% identification rate. This indicates that the load identification model employed herein possesses a robust load identification capability. At the same time, as shown in Table II, the proposed method achieves a high identification rate for loads with relatively simple operating states, such as fluorescent lamps, hair dryers, heaters, and vacuum cleaners. However, the identification rate is less ideal when dealing with loads with more complex operating states, such as air conditioners and refrigerators.

The figures on the main diagonal of the confusion matrix represent the precision of successful load identification; the larger the number, the higher the identification rate. It is evident from Fig. 5 that the model proposed in this study can effectively identify the majority of samples, with the recognition precision for samples such as fluorescent lamps, hair dryers, heaters, and vacuum cleaners reaching 100%.

TABLE II. EVALUATION METRICS FOR DIFFERENT APPLIANCES IN THE PLAID DATASET

Load Category	***Precision/%***	***Recall/%***	***F1-value/%***
Air Conditioner	94.2	94.2	95.4
Fluorescent Lamp	100	100	100
Electric Fan	97.3	97.3	96
Refrigerator	95.1	95.1	95.9
Hair Dryer	100	98.5	98.5
Heater	100	95.7	93.6
Incandescent Lamp	95.5	98.5	98.5
Laptop Computer	97.8	98.9	99.4
Microwave Oven	98	99	99.5
Vacuum Cleaner	100	100	99.2
Washing Machine Mean	95.7 97.6	97.8 97.7	96.8 97.5

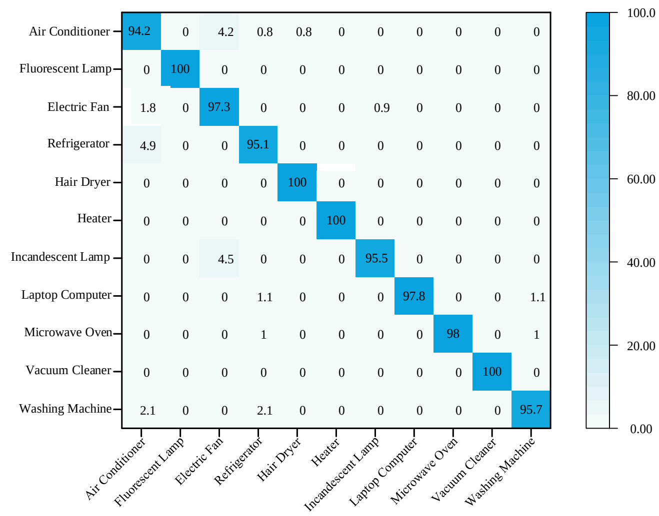

Fig. 5. Confusion matrix results of the PLAID data.

C. *Results of Field Measurements*

Several representative household loads were sampled via an intelligent load acquisition device. The utilized experimental apparatus is depicted in Fig. 6, comprising an experimental unit outfitted with an intelligent load control terminal that includes an integrated communication module. Additionally, the setup encompasses a cloud-based server where an automated demand response system is operational, a dedicated computer through which the user management interface is accessed, and a selection of electrical loads employed for testing purposes.

In a laboratory setting, data were collected for four types of electrical equipment: air conditioner, electric kettle, hair dryer, and laptop computer. Analyses were conducted on the performance of each equipment type when operated individually as well as in combination within a composite scenario, to ascertain the efficacy of the methodology proposed herein when applied to practical contexts. Table III presents the identification results for the different types of loads.

Fig. 6. The intelligent load collection device.

Several representative residential loads commonly used in daily life were selected for experimental validation. The method proposed herein achieves an identification rate of 100% for relatively simple resistive loads such as electric kettles and hair dryers, while maintaining an identification rate of over 94% for more complex loads such as air conditioners and laptop computers. A high identification rate is still retained for combinations of different types of loads, demonstrating the wide applicability of the proposed method in real-world scenarios.

TABLE III. LOAD IDENTIFICATION RESULTS IN EXPERIMENTAL SCENARIOS

Load type	*Identification precision/%*
Air conditioner	94.8
Electric kettle	100
Hair dryer	100
Laptop computer	95.9
Air conditioner+Electric kettle	96.1
Air conditioner+Laptop computer	96.5
Electric kettle+Laptop computer	97.6
Air conditioner+Electric kettle+Laptop computer	96.1

To further demonstrate the superiority of the load identification method proposed in this study, a comparison was made with various other load identification methods. Table IV presents the load signatures, training models, data sources, and experimental results used in this study and the other methods. Compared with other methods in Table IV, constructing WRG images and optimizing the AlexNet network can effectively improve the accuracy of load identification. However, when facing loads with more complex operating conditions, the identification rate will still be unsatisfactory.

TABLE IV. COMPARISON OF IDENTIFICATION RESULTS OF DIFFERENT METHODS

Method	*Load signature*	*Model*	*Dataset*	*Precision/%*
Literature [9]	Fused feature	BP	PLAID	91
Literature [10]	HSV color coding	AlexNet		94.6
Literature [15]	GMCE image	RBFNet	PLAID	92.1
			WHITED	91.1
Original AlexNet	WRG image	Original AlexNet	PLAID	94.3
			WHITED	95.1
			Field measurement	93.2
Proposed method	WRG image	Improved AlexNet	PLAID	97.6
			WHITED	98.1
			Field measurement	96.1

V. CONCLUSION AND FUTURE WORKS

A. Conclusion

The employment of WRG images for the color coding of the steady-state operational current of electrical apparatus has been demonstrated to possess greater feasibility over alternative methodologies. This is attributed to the singular requirement for current data acquisition, serving as the foundational data for load identification. Such a methodology considerably streamlines the data gathering process, thereby bolstering the practicality of the load identification endeavour.

This paper combines the image recognition method to achieve high-precision load identification, and identifies the load based on the improved AlexNet neural network, which greatly improves the load identification accuracy and the identification rate can reach more than 96%.

The proposed method can effectively encourage residential users to participate in demand response, thereby promoting the realization of the "double carbon" goal, and provides technical support for the construction of new power systems, and is suitable for practical promotion and use.

B. Future Works

In future endeavors, we will continue to convert one-dimensional time series data into two-dimensional image data using image encoding techniques, aiming to further refine the precision of the generated images. Additionally, we will concentrate on algorithmic optimizations for loads that exhibit multiple operating states, in order to meet the requirements for high-precision load identification in complex scenarios.

ACKNOWLEDGMENT

This work was supported by the Key Scientific Research Project of Colleges and Universities of Henan (No. 24A470006), the Science and Technology Project of Henan Province (No. 242102241027) and (No.24210221018， the Doctoral Scientific Research Foundation of Henan Polytechnic University (No. B2017-20).

REFERENCES

[1] Cui H, Wu Y, Jiang Y, Jiang C, Han T, Xu YP. Current sequence visualization method of non-intrusive load recognition. Electric Power Automation Equipment. 2022;42(7):40-45.

[2] Hart GW. Non-intrusive appliance load monitoring. Proc IEEE. 1992;80(12):1870-1891.

[3] Zhang L, Zhang T, Zhang HW. Research on a method of load identification based on multi parameter hidden Markov model. Power System Protection and Control. 2019;47(20):81-90.

[4] Gillis JM, Alshareef SM, Morsi WG. Nonintrusive load monitoring using wavelet design and machine learning. IEEE Trans Smart Grid. 2015;7(1):320-328.

[5] Gao J, Kara EC, Giri S, Bergés M. A feasibility study of automated plug-load identification from high-frequency measurements. In: 2015 IEEE Global Conference on Signal and Information Processing (GlobalSIP); 2015 Dec; Orlando, FL, USA. Piscataway (NJ): IEEE; 2015. p. 220-224.

[6] Figueiredo M, De Almeida A, Ribeiro B. Home electrical signal disaggregation for non-intrusive load monitoring (NILM) systems. Neurocomputing. 2012;96:66-73.

[7] Wang Z, Oates T. Encoding time series as images for visual inspection and classification using tiled convolutional neural networks. Workshops at the Twenty-Ninth AAAI Conference on Artificial Intelligence. Menlo Park, CA, USA; 2015.

[8] Wang Z, Oates T. Imaging time-series to improve classification and imputation. arXiv preprint arXiv:1506.00327. 2015.

[9] Lam HY, Fung GSK, Lee WK. A novel method to construct taxonomy electrical appliances based on load signatures. IEEE Trans Consum Electron. 2007;53(2):653-60.

[10] Hassan T, Javed F, Arshad N. An empirical investigation of VI trajectory based load signatures for non-intrusive load monitoring. IEEE Trans Smart Grid. 2014;5(2):870-8.

[11] De Baets L, Ruyssinck J, Develder C, Dhaene T, Deschrijver D. Appliance classification using VI trajectories and convolutional neural networks. Energy Build. 2018;158:32-6.

[12] Liu Y, Wang X, You W. Non-intrusive load monitoring by voltage–current trajectory enabled transfer learning. IEEE Trans Smart Grid. 2018;10(5):5609-19.

[13] Wang SX, Guo LY, Chen HW, Deng XY. Non-intrusive load identification algorithm based on feature fusion and deep learning. Autom Electr Power Syst. 2020;44(9):103-10.

[14] He D, Du L, Yang Y, Harley R, Habetler T. Front-end electronic circuit topology analysis for model-driven classification and monitoring of appliance loads in smart buildings. IEEE Trans Smart Grid. 2012;3(4):2286-93.

[15] Faustine A, Pereira L. Improved appliance classification in non-intrusive load monitoring using weighted recurrence graph and convolutional neural networks. Energies. 2020;13(13):3374.

[16] Gao J, Giri S, Kara EC, Bergés M. Plaid: a public dataset of high-resolution electrical appliance measurements for load identification research: Demo abstract. In: Proceedings of the 1st ACM Conference on Embedded Systems for Energy-Efficient Buildings; 2014. p. 198-199.

[17] Kahl M, Haq AU, Kriechbaumer T, Jacobsen HA. Whited-a worldwide household and industry transient energy data set. In: 3rd International Workshop on Non-intrusive Load Monitoring; 2016. p. 1-4.

[18] Chen J, Wang X, Zhang H. Non-intrusive load recognition using color encoding in edge computing. Chin J Sci Instrum. 2020;41(9):12-19.

[19] Wang AL, Chen BX, Wang CG, Hua D. Non-intrusive load monitoring algorithm based on features of V–I trajectory. Electric Power Syst Res. 2018;157:134-144.